Dalton Transactions

PAPER

View Article Online
View Journal | View Issue

Cite this: *Dalton Trans.*, 2016, **45**, 3327

Ionic liquid, glass or crystalline solid? Structures and thermal behaviour of $(C_4mim)_2CuCl_3$†‡

Philipp Zürner, Horst Schmidt, Sebastian Bette, Jörg Wagler and Gero Frisch*

Received 26th September 2015,
Accepted 9th January 2016

DOI: 10.1039/c5dt03772g

www.rsc.org/dalton

The ionic liquid $(C_4mim)_2CuCl_3$ was synthesised from a mixture of copper(I) chloride and 1-butyl-3-methylimidazolium chloride (C_4mimCl) and investigated using crystallographic and thermoanalytical methods. In the crystalline state, the compound consists of C_4mim^+ cations and triangular $[CuCl_3]^{2-}$ anions and forms three different modifications, which are connected through phase transitions at 227 and 203 K. The high and intermediate temperature phases crystallise in the space group *C*2, whereas the low temperature phase exhibits the space group $P2_1$. The three crystal structures are related through an isomorphic and a *klassengleiche* symmetry transition, respectively. The solid undergoes congruent melting at 320 K. The enthalpy of fusion was determined to be 25.7 kJ mol^{-1}. The melting process is irreversible and the ionic liquid can be supercooled to its glass transition at 221 K.

Introduction

Chloridometallate ionic liquids exhibit a rich structural chemistry, which can to a large extent be controlled by manipulating the composition of the melt.[1,2] This forms the basis for a large number of actual and potential applications, particularly in areas like catalysis, where precise control over important chemical properties, such as Lewis acidity, is essential.[3] Chloridocuprate ionic liquids in particular are interesting because of their redox behaviour and coordination chemistry and the catalytic properties associated therewith. With the cuprate complex as an integral part of the ionic liquid rather than a solute, these liquids show high catalytic activity under mild conditions or can bind large amounts of reactive gases. Consequently, they have been applied *e.g.* as catalysts,[4–6] precursors,[7] gas storage media[8] or extractants.[9] An advantage of Cu(I) based liquids is the chemical absorption of carbon monoxide *via* complexation, thus building copper carbonyl compounds that are catalytically active or can be used to recover carbon monoxide from gaseous streams.[10,11]

These compounds are readily prepared by mixing a chloride salt of an organic cation, in most cases an ammonium, phosphonium or imidazolium chloride, with either CuCl or $CuCl_2$. The key chemical parameter for most of the above applications is Lewis acidity, which can be adjusted by varying the ratio of organic and inorganic salts.[12] In a Lewis-neutral mixture, all copper ions are fully saturated with chloride but no free chloride ions are present in the melt. Accordingly, addition of excess chloride salt to this mixture results in a Lewis-basic melt whilst the addition of copper chloride leads to a Lewis acidic liquid with unsaturated or oligonuclear copper complexes.[8,10,13]

For mixtures of the commonly used ionic liquid 1-butyl-3-methylimidazolium chloride (C_4mimCl) with copper(II) chloride, the Lewis-neutral point is reached when the melt has the overall composition $(C_4mim)_2CuCl_4$. As expected, this mixture forms a stoichiometric compound in the crystalline state, containing $[CuCl_4]^{2-}$ ions.[14,15] Accordingly, dilute solutions of $CuCl_2$ in most chloride-based ionic liquids exhibit the same copper speciation.[16] Exceptions occur for cations with long alkyl chains, where singly charged anions are favoured.[2] For the analogue copper(I)-system, $[CuCl_2]^-$ has been proposed to be the anionic species in the Lewis neutral ionic liquid.[17,18] We have hence studied mixtures of C_4mimCl and CuCl at various compositions and found that the 2 : 1 mixture forms a stoichiometric compound: $(C_4mim)_2CuCl_3$. In the present study we were able to solidify this compound in a glassy state as well as three different crystalline phases. We discuss phase behaviour, crystal structures and crystallographic symmetry relations. Our findings suggest that the Lewis neutral species in these ionic liquids is probably $[CuCl_3]^{2-}$.

TU Bergakademie Freiberg, Institut für Anorganische Chemie, Leipziger Str. 29, 09599 Freiberg, Germany. E-mail: gero.frisch@chemie.tu-freiberg.de

† Electronic supplementary information (ESI) available. CCDC 1427586–1427588. For ESI and crystallographic data in CIF or other electronic format see DOI: 10.1039/c5dt03772g

‡ Dedicated to Professor Dr Wolfgang Voigt on the occasion of his 65th birthday.

Experimental

The chloridocuprate ionic liquid was formed by mixing 1-butyl-3-methylimidazolium chloride (C_4mimCl, Merck, anhydrous, for synthesis) and copper(I) chloride (Merck, for

Table 1 Lattice parameters of the crystalline phases of $(C_4mim)_2CuCl_3$. Values at 298 K have been obtained from XRPD, all others from single crystal XRD

			Unit cell parameters					
Phase	T/K	Space group	V/Å^3	Z	a/Å	b/Å	c/Å	β/°
High-T	298	$C2$ (no. 5)	1129.9(2)	2	13.032(1)	11.489(1)	8.398(1)	116.02(1)
	233		1113.8(9)		12.990(6)	11.404(4)	8.386(4)	116.30(3)
	Phase transition at 227 K							
Intermediate-T	213	$C2$ (no. 5)	2212.1(12)	4	12.983(4)	11.352(3)	15.982(5)	110.11(3)
	Phase transition at 203 K							
Low-T	90	$P2_1$ (no. 4)	2156.9(7)	4	12.854(2)	11.2524(13)	15.806(4)	109.355(16)

analysis) in a 2 : 1 molar ratio at 323 K. All synthetic experiments were carried out under argon (Praxair, 99.999%), which was dried over calcium chloride, to prevent hydrolysis and oxidation of Cu(I). The infrared spectrum of the melt as well as the crystalline solid at ambient temperature was recorded on a Nicolet 380 FT-IR spectrometer (Thermo Electron Corporation) and the spectra are shown in the ESI.†

The freezing point was determined in a Schlenk tube by cooling *ca.* 5 g of the liquid from 343 K to room temperature at a rate of 2 to 3 K min^{-1}. In the temperature range between 330 and 325 K, small seed crystals of $(C_4mim)_2CuCl_3$ were added every 20 s to prevent supercooling. Thermal effects were detected with a calibrated Teflon-coated type K thermocouple (Unitherm Messtechnik GmbH, data recording with TracerDAQ by Meilhaus Electronics) as a function of time.

Differential scanning calorimetry (DSC) was carried out using a TA Instruments DSC Q1000 with a refrigerated cooling system. Between 10 and 20 mg of the sample were sealed in aluminium crucibles in a glove box, transferred into the differential scanning calorimeter and analysed with heating/cooling rates of 1 and 2 K min^{-1}. All thermoanalytical experiments were carried out under dry nitrogen (Praxair, 99.999%). The data analysis of the thermoanalytical measurements was carried out with the onset tool of OriginPro 9.1G. Structural phase transition temperatures were reproducible within ±0.2 K, glass transition and melting point within ±0.5 K. The temperatures of the structural phase transitions are given as mean values of the onset values from heating and cooling runs.

Single crystal structures were determined with a STOE IPDS 2 T diffractometer using a Cobra cooling system and Mo-K_α (λ = 0.7107 Å) radiation. Crystals were separated from the bulk solid, encapsulated in a perfluorinated ether under a light microscope and transferred onto the goniometer in a stream of dry nitrogen. X-ray diffraction data were collected at temperatures between 80 and 250 K. Structure solution using direct methods with the SHELXS software yielded the position of all Cu, Cl and N as well as most of the C atom positions.[19] The positions of the remaining C atoms were located from difference Fourier maps during the refinement process. Least-squares refinement was carried out using the SHELXL programs.[19] All atoms except hydrogen were refined anisotropically. Electron density maps of the C_4mim^+ ions indicated disorder of the butyl groups. Simulated precession images were carefully checked for potential superstructure reflections but no such reflections could be found. The structures were hence refined using a disorder model where the occupancies of all atoms of the same butyl chain were constrained to the same value. Hydrogen atoms were refined in idealised positions. Pseudo symmetry elements B and C were detected by ADDSYM for the crystal structure at 90 K. ADDSYM uses the coordinates of the ordered structural model only. A lowering of the symmetry is caused mostly by the disordered atoms.

X-ray powder diffraction (XRPD) patterns were collected at room temperature on a laboratory powder diffractometer D8-Discover (Bruker), Cu-K_α radiation (λ = 1.5406 Å), from a primary Goebel Mirror monochromator, Vantac-1 detector (opening degree 1°, Bruker) in Bragg-Brentano geometry. The program TOPAS 4.2[20] was employed to determine the precise lattice parameters at ambient conditions. As the geometry of the Vantac-1 PSD is not fully characterized by Fundamental Parameters (FP),[21] the full instrumental peak profile was described with user defined 2θ-dependend Lorentzian-, Hat- and Circles convolutions that were determined by measurement of the NIST line profile standard SRM 660a (LaB_6) in Bragg-Brentano geometry over the 2θ range of the diffractometer. The background was modeled by employing Chebychev polynomials of 6th order. The precise lattice parameters (Table 1) were determined by Le Bail fits[22] using space group symmetry and initial values for the lattice parameters, a, b, c and β from the single crystal X-ray diffraction measurement at 233 K. Final agreement factors and fitting parameters of the Rietveld refinement are listed in the ESI.†

Results and discussion

General properties

The 2 : 1 mixture of C_4mimCl and CuCl formed a homogenous yellow liquid at 323 K. When cooled to room temperature, the mixture was still liquid after several weeks. During the cooling process, the liquid exhibited a significant increase in viscosity, which could be observed by the behaviour of the stirrer in the solution: whilst the liquid could be easily stirred with a magnetic stirrer at 323 K, an overhead stirrer was required at room temperature. This behaviour is typical for supercooled liquids.

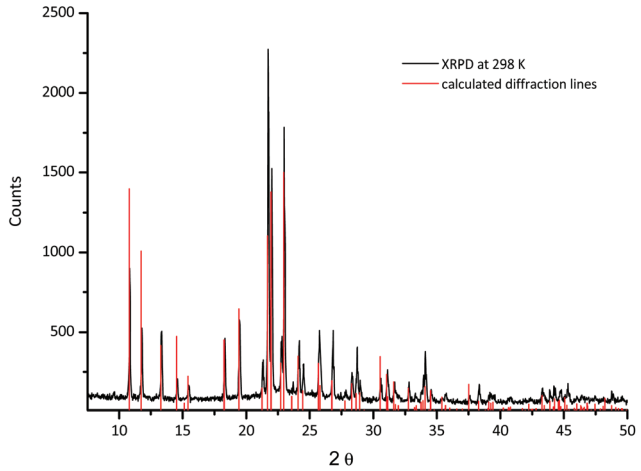

Fig. 1 X-ray powder diffraction pattern of $(C_4mim)_2CuCl_3$ (Cu-K_α) at ambient temperature. The simulated diffraction pattern was calculated using the 233 K crystal structure with refined lattice parameters for 298 K (see ESI†).

The crystallisation process was initiated by vigorous stirring of the mixture at 298 K with an overhead glass stirrer, whilst bubbling argon through the melt using a frit. After an hour, small crystals could be observed and the entire mixture solidified within 10 minutes, forming crystalline $(C_4mim)_2CuCl_3$. There was no indication of phase separation or impurities, and the XRPD pattern shows that the high temperature phase of $(C_4mim)_2CuCl_3$ was the only detectable crystalline phase (Fig. 1 and ESI†). Infrared spectra of the compound can be found in the ESI.†

When exposed to air for several minutes, the yellow solid $(C_4mim)_2CuCl_3$ forms a black slurry, which is typical for mixtures of copper(I) and copper(II) chlorides (Fig. 2). After several hours a green precipitate, possibly a copper(II) hydroxide, had formed on the surface. We conclude that $(C_4mim)_2CuCl_3$ is susceptible to both hydrolysis and oxidation and hence must be handled under an inert atmosphere at all times.

Phase behaviour

Before collecting variable temperature X-ray diffraction data sets from a single crystal, DSC measurements were carried out to investigate possible phase transitions. Sealed aluminium crucibles containing crystalline $(C_4mim)_2CuCl_3$ were cycled between room temperature and 193 K at various scan rates. All sets of temperature and enthalpy data obtained are identical within the experimental errors between heating rates of 1 and 2 K min^{-1}. Given values were derived from measurements with a scan rate of 1 K min^{-1}. Reversible signals could be observed at 227 and 203 K (Fig. 3), with a magnitude typical for structural phase transitions.[23] Due to the small temperature range of the two phase transitions, and therefore difficult peak separation, the transition enthalpy was determined through joint integration of both peaks. For the cooling and heating process, the overall transition enthalpy was found to be 2.5 and 2.9 J g^{-1}, respectively. Heating the sample further, a large endothermal signal corresponding to the melting point of $(C_4mim)_2CuCl_3$ was observed. The melting point was determined to be 320 K, using the onset method. The enthalpy of fusion was calculated from the peak area as 57.4 J g^{-1}, which corresponds to 25.7 kJ mol^{-1}, assuming $(C_4mim)_2CuCl_3$ as the formula unit. This is slightly higher than the enthalpy of fusion of pure C_4mimCl of 21 kJ mol^{-1}.[24]

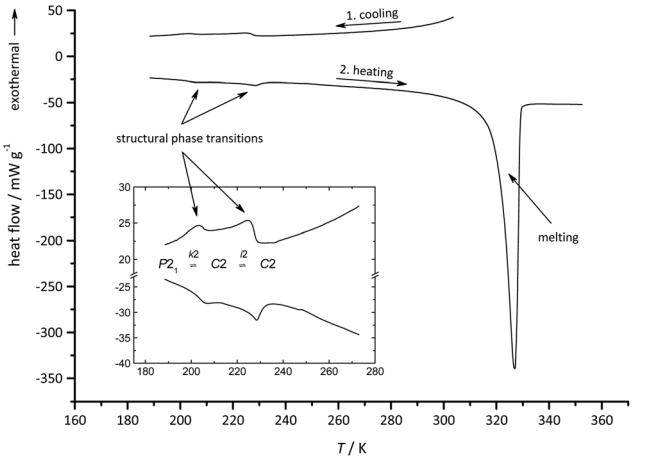

Fig. 3 DSC traces of $(C_4mim)_2CuCl_3$ crystals at a scan rate of 2 K min^{-1} showing two reversible solid–solid phase transitions at 227 and 203 K. The solid undergoes congruent melting at 320 K.

Fig. 2 Crystalline $(C_4mim)_2CuCl_3$ at ambient temperatures under inert atmosphere (l) and after being exposed to air for several minutes (r).

From macroscopic observations during the synthesis of the compound, the melting process is not expected to be reversible and the formation of supercooled phases is not uncommon in ionic liquids.[18,25] The crystallisation of highly viscous liquids is often inhibited due to the slow diffusion of the ions and insufficient crystal nucleation. Therefore, these compounds tend to supercool and eventually transform into a glassy state at temperatures which are often far below their melting point. The observed disorder of the butyl chains in the crystalline phases (see below) may also contribute to a retarded crystallisation process. As expected, no crystallisation peak could be observed in the DSC measurement when the sample was cooled from above the melting point. An ionic liquid of the overall composition $(C_4mim)_2CuCl_3$ can hence be regarded as a metastable liquid phase at room temperature.

To determine the freezing point of $(C_4mim)_2CuCl_3$, 5 g of the melt were slowly cooled in a Schlenk tube and the temperature was recorded as a function of time (Fig. 4). To avoid supercooling, the crystallisation was initiated by adding small seed crystals of $(C_4mim)_2CuCl_3$ when the melt had reached a temperature of 330 K. Crystallisation of the sample was accompanied by a slight increase in temperature and the temperature profile went through a plateau at 324 K. We hence treat the temperature value of this plateau as the freezing point of the compound.

When the sample is cooled to lower temperatures in the DSC experiment, no peaks occurred that would indicate a regular freezing point. At 221 K, a step in the heat flow was observed, which is indicative of a glass transition. The glass transition temperature was determined as the inflexion point of the step in the DSC curve (Fig. 5). During glass formation, the heat capacity changes from 1.1 to 0.7 J g^{-1} K^{-1}.

The glass transition was always accompanied by exothermal signals, which occurred between 218 and 209 K, depending on the cooling rate. The peak area was relatively small and, depending again on scan rate, corresponded to an enthalpy between 0.1 to 0.7 J g^{-1}. This could indicate that a small fraction of the sample is crystallising whilst the majority is transformed into the glassy state. On the heating branch of the DSC measurement, the glass transition occurred at 222 K, which is comparable to the values given in the literature for similar compounds.[18] At a heating rate of 2 K min^{-1}, no further signals are observed after the glass transition. However, at 1 K min^{-1} a large exothermal signal occurred at 267 K (Fig. 6) with a peak area corresponding to an enthalpy of 22.1 kJ mol^{-1}. This is similar to the enthalpy of fusion and the signal at 267 K is probably caused by the crystallisation of $(C_4mim)_2CuCl_3$ from the supercooled liquid. This observation

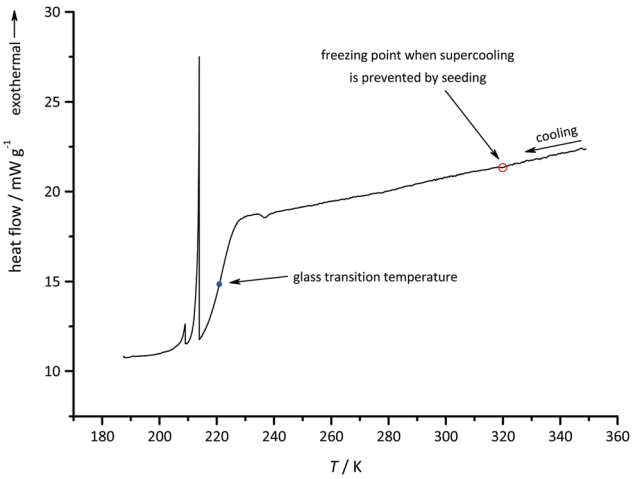

Fig. 5 DSC cooling trace of molten $(C_4mim)_2CuCl_3$ (1 K min^{-1}). No crystallisation is observed (red circle). A glass transition occurs at 221 K (blue circle). Small exothermal signals are probably due to a small fraction of the sample crystallising, whilst the majority is transformed into the glassy state.

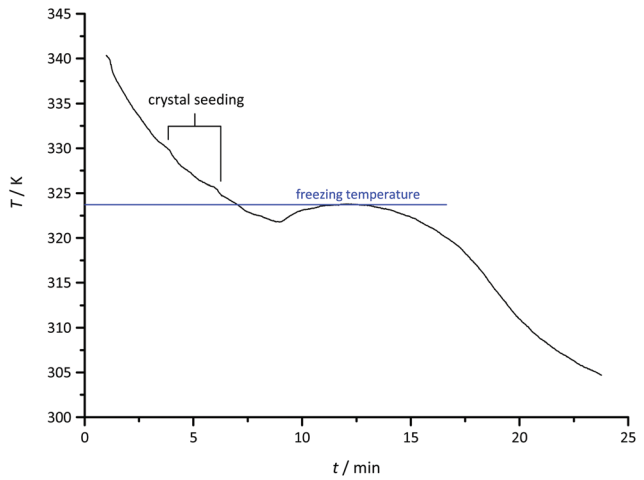

Fig. 4 Thermal effects of molten $(C_4mim)_2CuCl_3$ in a Schlenk tube upon cooling. Supercooling was avoided by adding small seed crystals of $(C_4mim)_2CuCl_3$ at 330 K. Freezing was observed at 324 K.

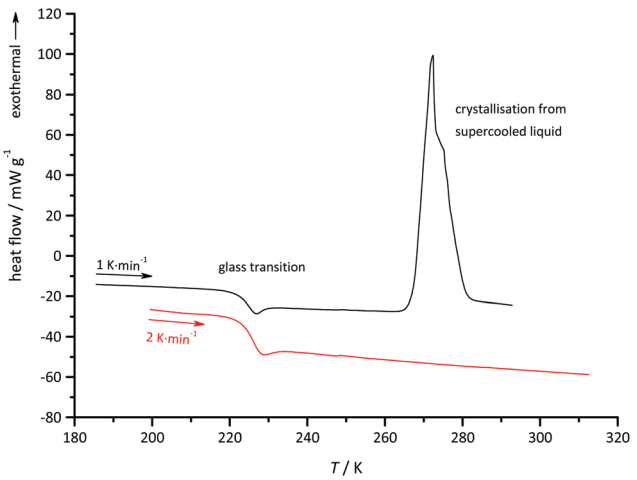

Fig. 6 DSC heating traces of $(C_4mim)_2CuCl_3$. At the slower scan rate crystallisation occurs from the supercooled liquid at 267 K.

is in support of our hypothesis that a small fraction of the sample is crystallising during glass transition. This could lead to the formation of seed crystals, which initiate crystallisation of the supercooled melt upon heating, whereas crystallisation had been inhibited in the cooling process.

Crystal structures

DSC measurements showed that there are three different crystalline phases, which have similar lattice energies and are probably connected through structural phase transitions. Accordingly, using single crystal X-ray diffraction, three different crystal structures could be obtained at 233 K, 213 K and 90 K which are henceforth called high, intermediate and low temperature phases. The three phases exhibit very similar crystal structures, which are closely symmetry-related. This is consistent with the small phase transition energies observed in the DSC experiments. Crystallographic data are shown in Table 1 and the ESI.†

The XRPD-pattern of the bulk material confirms that the high temperature phase was formed in the crystallisation experiments under ambient conditions. There is an offset between the calculated diffraction lines of the 233 K data set and the ambient temperature XRPD, which increases with the diffraction angle (diffractogram in ESI†). This is to be expected, due to the temperature dependence of the lattice parameters. A Rietveld refinement of the powder pattern (Fig. 1) based on the structural data of the 233 K data set confirmed the identity of this phase in the bulk material at room temperature. The refined lattice parameters of $(C_4mim)_2CuCl_3$ at 298 K and all lattice parameters for the single crystal structures are shown in Table 1.

All three phases consist of triangular $[CuCl_3]^{2-}$ anions and twice as many C_4mim^+ cations. The molecular formula can be hence described as $(C_4mim)_2CuCl_3$, which is identical with the overall composition of the melt the compound was crystallised from. The high temperature unit cell contains two of these formula units, whilst the intermediate and lower temperature phases exhibit almost twice the unit cell volume and consequently contain four formula units.

The asymmetric unit of the high temperature phase is shown in Fig. 7. The copper atoms are coordinated by three chlorine atoms resulting in $[CuCl_3]^{2-}$ in a planar coordination geometry. Cu–Cl distances are 2.219(3) and 2.255(2) Å, which is typical for Cu(I)–Cl bonds. Cl–Cu–Cl bond angles are 115.06(11)° and 122.47(6)°. For the high temperature phase, all butyl carbon atoms of the imidazolium cation are disordered, which is commonly observed in these kinds of compounds due to the flexibility of the alkyl chain.[14] The relative occupancy of the two sets of positions was refined to a values of 0.38(2) and 0.62(2), respectively. With decreasing, temperature the alkyl chain becomes less disordered.

For the ion packing, C–H···Cl contacts seem to be an essential factor as the cations and anions are linked by multiple C–H···Cl interactions. The H···Cl distances vary between 2.58 and 2.97 Å (Fig. 8) which is consistent with the values found in the literature.[13,26] As expected, the shortest of these contacts,

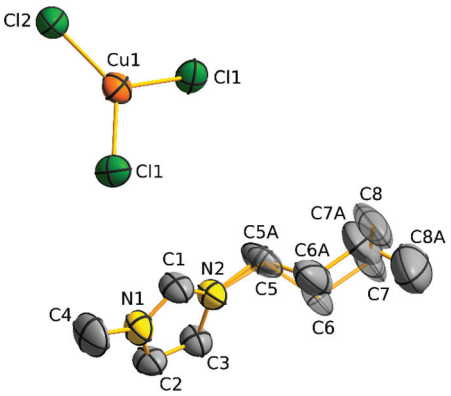

Fig. 7 Asymmetric unit of the high temperature phase of $(C_4mim)_2CuCl_3$ with disordered butyl residue. Relative occupancy CXA : CX = 0.62 : 0.38(2). Hydrogen atoms are omitted for clarity.

with a H1···Cl1 distance of 2.584(5) Å, is formed by the most acidic proton, which belongs to the CH-group in the 2-position of the imidazolium core. This is in good agreement with the crystal structure of the analogue chloridocuprate(II) ionic liquid $(C_4mim)_2CuCl_4$ where the shortest H···Cl distance was determined to be 2.50 Å.[14] The other contacts vary in length with a clear gap in the list of H···Cl distances around 3 Å. Accordingly, Fig. 8 shows the interactions between the complex anion and the imidazolium unit with 2.973(4) Å as the longest C–H···Cl contact.

Considering these C–H···Cl interactions, the structure can be described as a molecular network with $[CuCl_3]^{2-}$ anions being staggered along all three crystallographic axes (Fig. 9). The C_4mim^+ cations are aligned between the anions with alter-

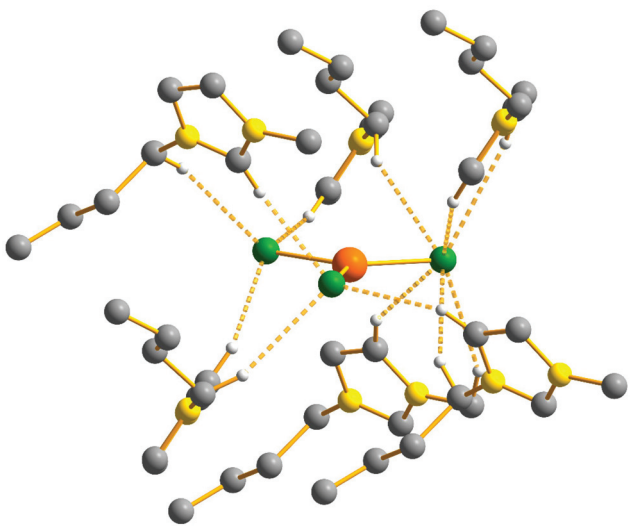

Fig. 8 C–H···Cl contacts of planar $[CuCl_3]^{2-}$ anions and C_4mim^+ cations up to 2.97 Å. Disordered atoms and hydrogen atoms not involved in C–H···Cl contacts have been omitted for clarity.

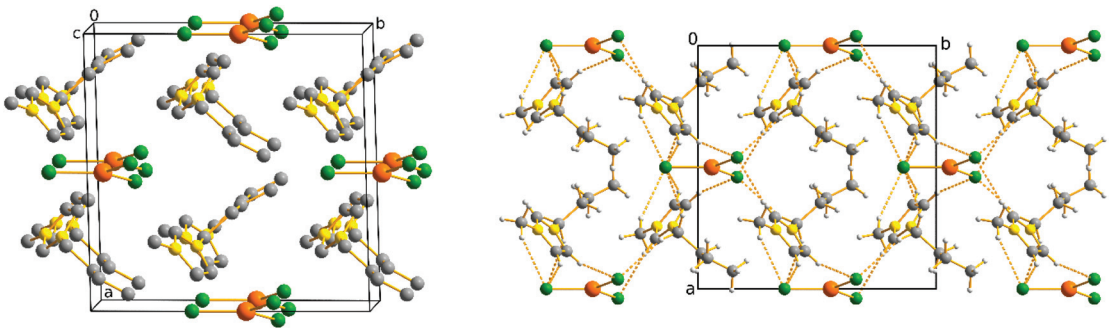

Fig. 9 Unit cell of the high temperature phase of $(C_4mim)_2CuCl_3$ (l). Molecular network with $[CuCl_3]^{2-}$ anions staggered along all three crystallographic axes and C_4mim^+ cations aligned with alternating orientation, avoiding steric interaction of the alkyl chains (r).

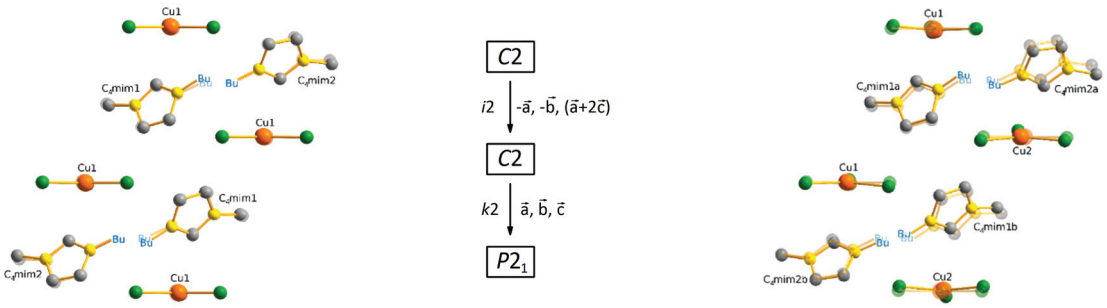

Fig. 10 Symmetry transitions of $(C_4mim)_2CuCl_3$: high (transparent) to intermediate temperature phase (l); intermediate (transparent) to low temperature phase (r). Butyl chains (Bu) and hydrogen atoms have been omitted for clarity.

nating orientation, avoiding steric interaction of the alkyl chains.

Upon lowering the temperature, a structural phase transition occurs at 227 K, according to the DSC measurements. In the course of this transformation the planes formed by the chlorine atoms, which were parallel in the high temperature structure, are tilted by 2.63° with respect to each other. The imidazolium moieties are shifted accordingly, resulting in two crystallographically independent cations (Fig. 10, left). These are still positioned with alternating orientation but, due the tilts and shifts described above, the cell volume has doubled. The two structures are related through an isomorphic symmetry transition of index 2 within the same space group *C*2.

The results from the DSC measurements indicate a second phase transition at 203 K. Upon decreasing temperature to 90 K the structure undergoes a *klassengleiche* symmetry transition of index 2 to the spacegroup $P2_1$, resulting in two crystallographically independent cuprate ions and four independent imidazolium moieties (Fig. 10, right). The tilt between the cuprate anions increases to values between 3.95 and 15.33°. Nevertheless, the displacement of the copper atom out of the planar Cl_3 coordination sphere is relatively small with a maximum value of 0.0447(5) Å. Whilst symmetry reduction is occurring from the high to the low temperature structure, the disorder of the butyl chain is lowered with decreasing temperature, as expected.

The symmetry relations, including coordinate transformation for all non-disordered atom positions, are given in the ESI.†

Conclusions

The general properties of a 2 : 1 molar mixture of C_4mimCl and CuCl were studied and crystallisation of $(C_4mim)_2CuCl_3$ could be achieved. We studied the thermoanalytical properties of this new compound and determined three different crystal structures. DSC measurements indicate two reversible solid–solid phase transitions at 227 and 203 K. The melting point was determined to be 320 K and the corresponding enthalpy of fusion is 25.7 kJ mol^{-1}. With decreasing temperature, no crystallisation could be observed in the DSC measurement due to extensive supercooling of the melt. The freezing point could only be obtained by the addition of small seed-crystals during the cooling process and was found to be 324 K, which is in good agreement with the melting point derived from the DSC measurement data. Without the addition of $(C_4mim)_2CuCl_3$ crystals, the liquid transforms into a glassy state at 221 K. This process is accompanied by small exothermic effects, probably due to the crystallisation of a small fraction of the sample.

Through single crystal X-ray diffraction measurements within the stability range of the three different crystalline phases, the crystal structures of these phases could be determined. They exhibit similar structures, which are related through an isomorphic and a *klassengleiche* symmetry transition of index 2. X-ray powder diffraction measurements of the bulk material show that the high temperature phase found by single-crystal structure analysis is the only phase present at ambient temperatures. All crystal structures consist of planar $[CuCl_3]^{2-}$ anions and twice as many C_4mim^+ cations. These are linked *via* multiple C–H···Cl contacts, ranging from 2.58 to 2.97 Å, building a molecular network. The C_4mim^+ cations are aligned with alternating orientation between the staggered $[CuCl_3]^{2-}$ anions to avoid steric interaction of the butyl chains. The butyl moiety of the imidazolium cation is disordered in all three crystal structures due to the flexibility of the alkyl chain. With decreasing temperature, the planes formed by the chlorine atoms tilt, causing the imidazolium molecules to rearrange, hence lowering the symmetry of the crystal structures. The tilting of the complex anions has only a marginal effect on the planar coordination of the copper(I) atoms.

Acknowledgements

The authors would like to thank Regina Moßig and Iris Paschke for support with the DSC and XRPD measurements, respectively.

References

1 J. Estager, J. D. Holbrey and M. Swadzba-Kwasny, *Chem. Soc. Rev.*, 2014, **43**, 847.
2 J. M. Hartley, C.-M. Ip, G. C. H. Forrest, K. Singh, S. J. Gurman, K. S. Ryder, A. P. Abbott and G. Frisch, *Inorg. Chem.*, 2014, **53**, 6280.
3 A. A. Fannin Jr., D. A. Floreani, L. A. King, J. S. Landers, B. J. Piersma, D. J. Stech, R. L. Vaughn, J. S. Wilkes and J. L. Williams, *J. Phys. Chem.*, 1984, **88**, 2614.
4 M. Stricker, T. Linder, B. Oelkers and J. Sundermeyer, *Green Chem.*, 2010, **12**, 1589.
5 J. Pavlinac, M. Zupan, K. K. Laali and S. Stavber, *Tetrahedron*, 2009, **65**, 5625.
6 H. Zhao, J. E. Holladay, H. Brown and Z. C. Zhang, *Science*, 2007, **316**, 1597.
7 A. Taubert, *Angew. Chem., Int. Ed.*, 2004, **43**, 5380.
8 D. J. Tempel, P. B. Henderson, J. R. Brzozowski, R. M. Pearlstein and H. Cheng, *J. Am. Chem. Soc.*, 2008, **130**, 400.
9 X. Chen, D. Song, C. Asumana and G. Yu, *J. Mol. Catal. A: Chem.*, 2012, **359**, 8.
10 O. C. David, G. Zarca, D. Gorri, A. Urtiaga and I. Ortiz, *Sep. Purif. Technol.*, 2012, **97**, 65.
11 G. Zarca, I. Ortiz and A. Urtiaga, *J. Membr. Sci.*, 2013, **438**, 38.
12 C. Nanjundiah and R. A. Osteryoung, *J. Electrochem. Soc.*, 1983, **130**, 1312.
13 H. Sun, K. Harms and J. Sundermeyer, *Z. Kristallogr.*, 2005, **220**, 42.
14 C. Zhong, T. Sasaki, A. Jimbo-Kobayashi, E. Fujiwara, A. Kobayashi, M. Tada and Y. Iwasawa, *Bull. Chem. Soc. Jpn.*, 2007, **80**, 2365.
15 S. Caporali, C. Chiappe, T. Ghilardi, C. S. Pomelli and C. Pinzino, *ChemPhysChem*, 2012, **13**, 1885.
16 A. P. Abbott, K. El Ttaib, G. Frisch, K. J. McKenzie and K. S. Ryder, *Phys. Chem. Chem. Phys.*, 2009, **11**, 4269.
17 D. D. Axtell, B. W. Good, W. W. Porterfield and J. T. Yoke, *J. Am. Chem. Soc.*, 1973, **95**, 4555.
18 S. A. Bolkan and J. T. Yoke, *J. Chem. Eng. Data*, 1986, **31**, 194.
19 G. M. Sheldrick, *Acta Crystallogr., Sect. A: Found. Crystallogr.*, 2008, **64**, 112.
20 *Bruker AXS Topas, version 4.2*, 2009.
21 R. W. Cheary, A. A. Coelho and J. P. Cline, *J. Res. Natl. Inst. Stand. Technol.*, 2004, **109**, 1.
22 A. Le Bail, H. Duroy and J. L. Fourquet, *Mater. Res. Bull.*, 1988, **23**, 447.
23 G. Höhne, *Differential scanning calorimetry. An introduction for practitioners; with 13 tables*, Springer, Berlin, 1996, p. 108.
24 T. Endo, T. Kato and K. Nishikawa, *J. Phys. Chem. B*, 2010, **114**, 9201.
25 M. Yoshizawa, A. Narita and H. Ohno, *Aust. J. Chem.*, 2004, **57**, 139.
26 M. L. Glowka and G. Gilli, *Acta Crystallogr., Sect. C: Cryst. Struct. Commun.*, 1989, **45**, 408.